THE ARCHIVES OF TRANSPORT
VOL. XXII NO 1 2010
10.2478/v10174-010-0002-5

On Some Corrugation Related Dynamical Problems of Wheel/Rail Interaction

Roman Bogacz*
Kurt Frischmuth**

Received November 2009

Abstract

We simulate the motion of a corrugated disk over a corrugated track under unilateral elastic contact forces. In particular, the trajectory of the geometrical contact point and the magnitude of normal forces are studied. Effects like generation of waves and cumulation of plastic deformation are considered.

Keywords: railway mechanics, contact geometry, friction, bouncing, wave generation, plastic deformation

1. Introduction

In a series of previous papers the behavior of simple models of railway vehicles was studied with special regard to the frictional power dissipated in the contact region, [2, 3, 8, 11-16].

The aim of most of those studies was the calculation of wear leading to poligonalization, which is mostly caused by abrasion.

In a number of previous papers devoted to the dynamics of periodical structures under a moving force various types of oscillations were studied, [10], [11]. Some investigations were devoted to the analysis of the development of corrugations using linear and non-linear wheel/rail interaction models. A rigid and an elastic contact model were discussed in [12], elastic and perfect plastic models were studied in

* Institute of Fundamental Technological Research Polish Academy of Sciences, Pawińskiego 5B Str., 02-106 Warsaw; Tadeusz Kościuszko Cracow University of Technology, Warszawska 24 St., 31-155 Kraków, Poland
** Universitat Rostock

[13], and a discussion of frictional wear as source of surface pattern development in rolling contact is given in [15]. Similarly as in the approach made by Kowalska [15], [16], we will study the two-dimensional problem with jumps of wheel/rail contact and inelastic impacts.

Typical corrugations, also called slip-waves, have a much smaller wave length, and are believed to be related to percussional effects leading to permanent (plastic) deformations of the surface layer. Analysis of the contact geometry of rigid bodies with harmonic corrugations shows that already at comparatively low speeds two effects may be observed.First, the point of geometrical contact moves forth and back around the actual position of the wheel. Thus we have to deal with a force traveling at variable speed. Due to large amplitudes of the speed, critical regions of speeds are crossed, see [11].

Another interesting topic concerning the interaction between wheel and rail is connected with the fact that during the rolling process on a wavy pattern the speed of the contact area is oscillating around the value of the lateral velocity of the wheel center. The critical value of the speed is connected with the velocity of elastic wave propagation in the rail or wheel tyre.

At this velocity begins a process of rapid plastic deformation due to increase of contact forces [11]. Such kind of phenomena are responsible for the development of corrugations.

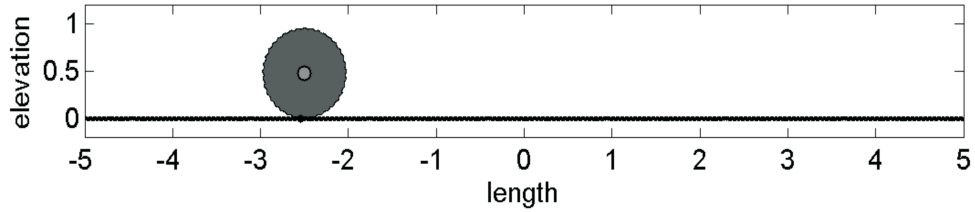

Fig. 1. Segment of track and wheel, both corrugated (amplitudes exaggerated, 5 mm on rail, 7 mm on wheel)

2. Geometry

2.1. Constraints

In previous works, the motion of an ideal wheel over a wavy track was considered, cf. [1, 4, 5, 13]. A pure geometric study of contact geometry results in constraints which do not depend on the angle of revolution of the wheel.

Here, however, we have the problem of two corrugated surfaces, see Fig. 1, hence we need to determine for each angle and each horizontal position of the wheel center the lowest vertical position such that contact occurs. We do this by studying the gap between the contact partners, looking for the minimizer, cf. Fig. 3.

The minimizer, as function of angle of revolution and horizontal position, is the geometrical point of contact, the value of the minimum gives the constraint for the elevation of the wheel center.

We assume ideal periodicity of the corrugation pattern. This will allow later to reduce the numerical costs. In general, we have to consider superposition of several modes or use e.g. spline approximation of the surfaces.

For the rail, we set

$$y_r(x; a_r, \omega_r) = a_r \sin(2\pi\omega_r x) \tag{1}$$

while the wheel geometry, a sinusoidal perturbation of the radius is postulated

$$\begin{aligned} r(\varphi; a_\mathrm{w}, \omega_\mathrm{w}) &= R_0 + a_\mathrm{w} \sin(\omega_\mathrm{w}\varphi), \\ x_\mathrm{w}0(\varphi; a_\mathrm{w}, \omega_\mathrm{w}) &= r(\varphi; a_\mathrm{w}, \omega_\mathrm{w}) \cos(\varphi) + R_0, \\ y_\mathrm{w}0(\varphi; a_\mathrm{w}, \omega_\mathrm{w}) &= r(\varphi; a_\mathrm{w}, \omega_\mathrm{w}) \sin(\varphi). \end{aligned} \tag{2}$$

For simulations, we use the parameters given in Tab. 1 and Tab. 2.

Table 1

Track parameters

length	10 m
wave length	0.05 m
amplitude	1.25e-4 m
number of waves	200

Table 2

Wheel parameters

radius	0.47 m
wave length	0.08 m
amplitude	1e-4 m
number of waves	37

For this paper, we assume the rail position to be frozen, the wheel is mowing as a rigid body – except for very localized elastic deformations in the vicinity of the contact point. The actual wheel circumference is obtained from the reference shape defined above by rotation (revolution) and shift (translative motion, mostly horizontal)

$$\begin{pmatrix} x_w(t) \\ y_w(t) \end{pmatrix} = \begin{pmatrix} \cos(\alpha(t)) & -\sin(\alpha(t)) \\ \sin(\alpha(t)) & \cos(\alpha(t)) \end{pmatrix} \begin{pmatrix} x_w 0 \\ y_w 0 \end{pmatrix} \begin{pmatrix} x(t) \\ y(t) \end{pmatrix} \tag{3}$$

For an ideal wheel, we have a constant curvature $\kappa = 1/\mathrm{R}_0$, in the perturbed case, κ oscillates in a nearly harmonic way, cf. Fig. 2. As we will see later, only for

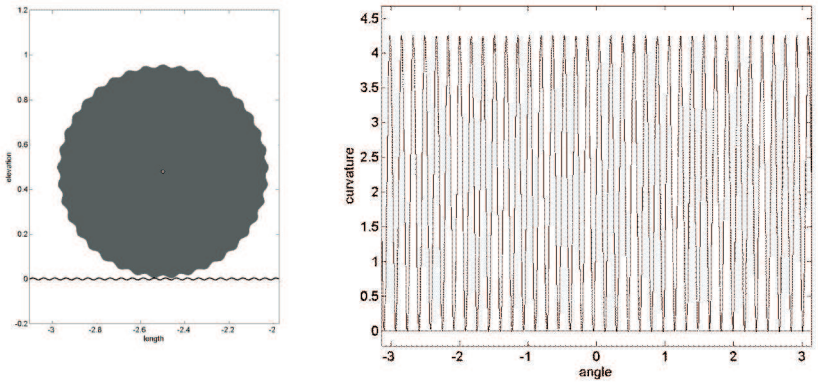

Fig. 2. Corrugated wheel and its curvature

small amplitudes, $\kappa(\phi$ stays positive for all angles ϕ. A violation of this condition, however, leads to multiple contact even on ideal track.

A convenient tool for the study of multiple geometric contact is the gap function. There are several choices of how to measure and how to parametrize the gap. We base our calculations on the wheel parameter φ, for each parameter we evaluate the x_w–coordinate, get $y_r(x_r)$ and take the difference $g(\varphi;\, x,\, \alpha) = y_w\ (\varphi;\, x,\, \alpha) - y_r(x_r\ (\varphi;\, x,\, \alpha)) + g_0$. The constant $g_0(x,\, \alpha)$ is to be chosen in such a way that $\min\ \varphi \in [0.2\pi] g(\varphi) = 0$.

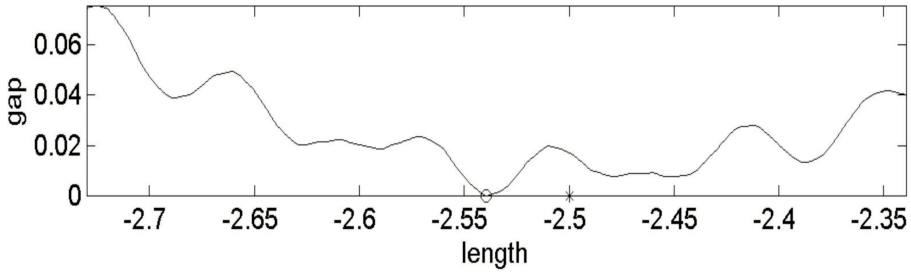

Fig. 3. Gap between rail and wheel

Notice that this is not the perpendicular distance from a point on the wheel's circumference to the closest point on the rail, assuming the rail is corrugated. For true rigid body motion, we have the unilateral constraint $y(t) \geq g_0(x(t),\, \alpha(t))$.

For starters, we do some of the calculations for a corrugated wheel on an ideal track surface. However, in most cases both surfaces are corrugated. We show here the dependence of vertical elevation of the wheel center and the contact point's relative horizontal position with respect to the wheel center in dependence of the angle of

revolution and the abscissa of the wheel center. Due to the assumed periodicity of both contact partners, we need only present a periodicity cell.

In Fig. 4, we show what happens for very moderate amplitudes, a_r = 0.2 mm, a_w = 0.1 mm (all other parameters as before).

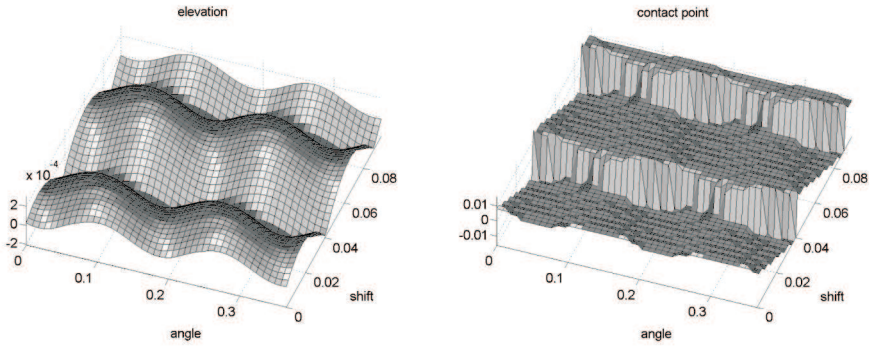

Fig. 4. Elevation and contact shift for both partners corrugated

2.2. Contact Point

The point of contact is defined as $(x_c, y_c)^T = (x_w(\varphi_c), y_w(\varphi_c))^T$, where φ_c denotes the minimizer of g. The latter, in general, is not unique, hence we may have multiple points of contact. In fact, in such situations a further index should denote which point from the contact set is considered.

In the case of an ideal track, multiple contact is impossible as long a the wheel remains convex. Fig. 2 shows the limit case – for the given wave number of 37 and the critical amplitude of corrugations of 0.34 mm, curvature begins to change sign. The result is multiple contact – and hence bouncing of the wheel.

$$\kappa_{\text{ideal}} = 1/R_0, \kappa_{\min_{\sin}} = -1, \kappa_{\min_{a\sin(\omega\cdot)}} = -a(\omega/R_0)^2 \tag{4}$$

The condition for convexity reads:

$$a \leq R_0/\omega^2 \tag{5}$$

In the case of both partners featuring corrugations, multiplicity of contact points depends on the relative position of the bodies with respect to each other.

We confirmed that the above rather rough estimate is consistent with the full analytical evaluation of the curvature and neglecting higher order terms as well as with a straightforward numerical test of convexity. For both surfaces corrugated, in a similar way a sufficient condition for uniqueness of the geometrical contact point may be derived. We impose the condition that the gap is a convex function, and we

estimate the second derivative of the gap function by the difference of minimum wheel curvature minus maximum rail curvature.

For this difference positive, no multiple contact may occur.

The mean value of the wheel curvature is obviously $\kappa_{\text{mean}} = 1/R_0$. For the assumed perturbation imposed on the ideal constant radius $\Delta_w = a_w \sin(\omega_w \varphi)$, the second derivative is $-a_w \omega^2 \sin(\omega_w \varphi)$ and has a minimum value of $a_w \omega^2$. This is the second derivative with respect to the angle, what we need is the corresponding value with respect to arc length.

Scaling via $\varphi \to R_0 \varphi$ leads finally to the approximation

$$\kappa = \kappa_{\text{mean}} - a_w \omega^2 \sin(\omega_w \varphi)/R_0^2 \tag{6}$$

Critical for contact are points of minimal radius, hence we calculate the curvature κ there and obtain the condition

$$\frac{1}{R_0} - a_w \frac{\omega_w^2}{R_o^2} \geq 0 \tag{7}$$

$$a_w \leq \frac{R_0}{\omega_w^2} \tag{8}$$

For $R_0 = 0.5$, $\omega_w = 40$, $a_w \leq 0.5/1600 \approx 0.3\text{E-}3$.

For the rail surface, we assume a perturbation of the form

$$\Delta_r = a_r \sin(\omega_r s 2\pi) \tag{9}$$

$$\kappa_r = -a_r \omega^2 \sin(\omega_r s 2\pi) \tag{10}$$

which amounts to ω_r humps per unit of length.

Hence, a sufficient condition for an easy ride – without multiple contacts – is

$$\min \kappa_w > \max \kappa_r \tag{11}$$

$$\frac{1}{R_0} - a_w \frac{\omega_w^2}{R_o^2} > 4 a_r \omega_r^2 \pi^2 \tag{12}$$

or simply

$$4\pi^2 R_0^2 a_r \omega^2 + a_w \omega^2 < R_0 \tag{13}$$

We conclude that for given wave lengths of the perturbation, the admissible range for the amplitudes is a triangle.

For given amplitudes, the the domain for frequencies is bounded by an ellipse.

3. Forces

The pure geometric approach leads to a mechanical system with kinematic constraints, which are enforced by Lagrange multipliers. The latter can not be calculated from the position coordinates and velocities alone, they result from the solution of the system of equations of motion.

As an alternative, a stiff elastic system may be formulated, for which violation of the contact condition – in the form of a penetration of the undeformed shapes of the contact partners – is penaltized by a normal force, e.g. Winklerian or Herzian.

Both approaches allow a unilateral treatment, i.e., positive vertical gaps may be allowed. In time intervals, where this occurs, we have a free flight of the wheel – which ends with an impact.

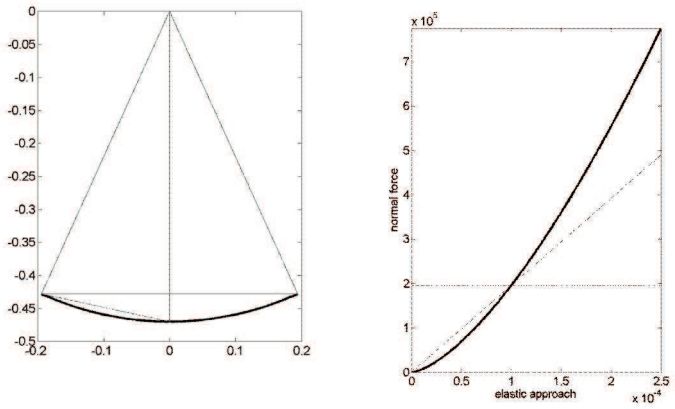

Fig. 5. Contact geometry and normal forces

Lateron we will assume a load of around 20t on our wheel, which has a radius of about half a meter. A typical contact patch has a length of around 1 to 2 cm.

Fig. 5, left part shows that this is compatible with an elastic approach of around one tenth of a mm.

Indeed

$$\Delta y = R_0 - \sqrt{R_0^2 - \left(\frac{l}{2}\right)^2} \tag{14}$$

We obtain the parameter used for calculations for l = 0.02, R_0 = 0.47. The quasi-static normal force resulting according to Herzian theory is depicted in Fig. 5, right part.

In order to find a reasonable damping, let us bounce a wheel vertically onto a perfect (straight) rail – without horizontal motion. We show results for d = 1e4,

d = 1e5, d = 4e5, d = 1e6 (in Ns/m). The result for d = 4e5 is consistent with experimental evidence, see Fig. 6.

We have to remember that the contact stiffness according to Herz depends on the difference between curvatures. So further refinement is required here.

The continuous curves correspond to a linear contact spring, the dashed ones to Herzian contact. The differences are rather only quantitative.

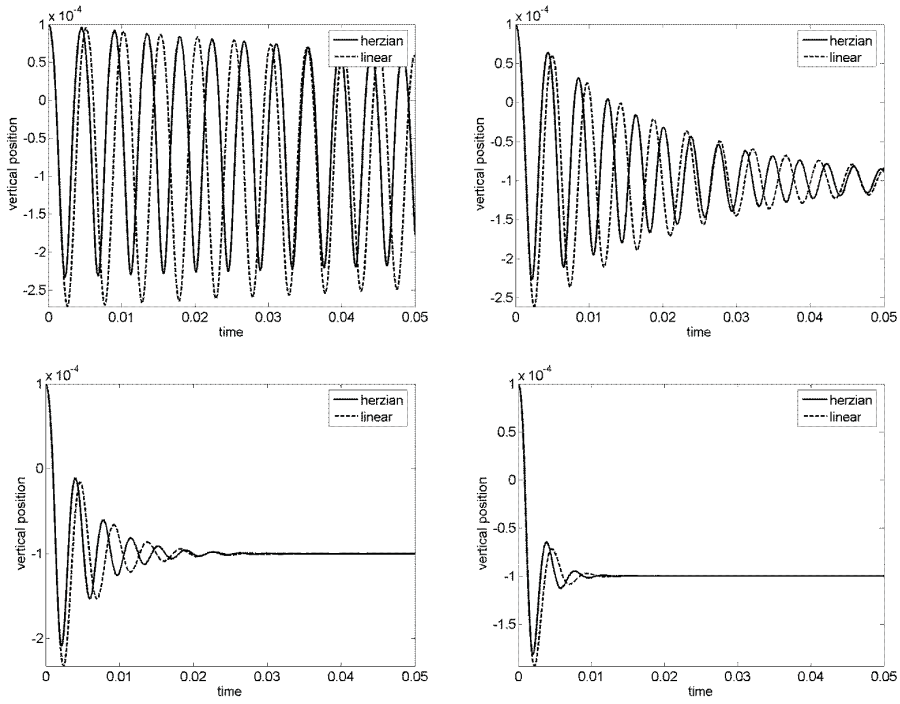

Fig. 6. Normal oscillations for various damping

4. Simulations

4.1. Ideal Rolling

We start with a simple kinematical consideration. Assume the center of wheel moves at a prescribed speed.

Further, assume that both bodies are rigid, and they are at all times in contact in a uniquely defined point of geometrical contact.

Finally, at the point of contact there is no relative motion between wheel and rail, which amounts to the condition that the velocity of the contact point on the wheel circumference is zero.

The above conditions define the trajectory of the wheel center and the revolution of the wheel uniquely. Hence, we obtain vertical acceleration and angular moment and thus normal force and frictional force in tangential direction.

Remark 1 *Under such idealized conditions of contact, friction and rolling, we may calculate position and vertical force in the the contact point without solving the equations of motion.*

We derive from this a new type of traveling force problem

$$F_y(t, x) = (F_0 + F_1 \sin(c_1 t)) \cdot \delta(x_0 + V_0 t + x_1 \sin(c_2 t + c_3) - x) \tag{15}$$

What is new is the oscillation of the force position around its mean position which moves steadily forward.

Critical speeds and frequencies have been derived for the case $x_1 = 0$. The oscillating position may exceed the critical speed, but only on small intervals. The effects of this need further considerations.

4.1.1. Relation Between Loci of Wheel Center and Contact Point

Assume an ideal disk wheel and wavy rail surface.

It is straightforward to create a parametrization of the wheel center locus in terms of the horizontal coordinate of the contact point as parameter. We have to perform a vector addition of the (contact) point (x_c, y_c) on the rail with horizontal coordinate s and the normal vector $(-r'(s), 1)$ multiplied by the wheel radius R_0. The resulting curve may be non-smooth or even contain loops. True rolling – withcontinuous one-point contact – is only possible as long as the curve is free of double-points.

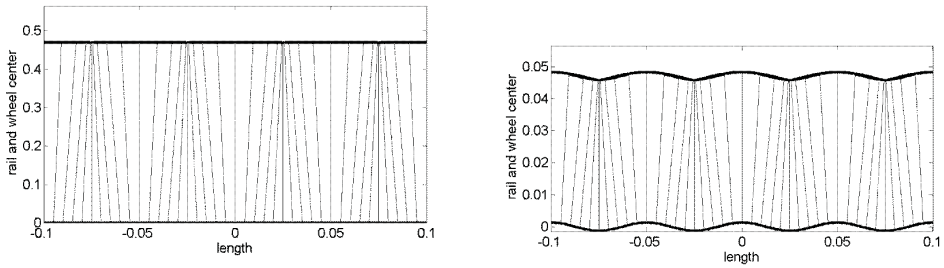

Fig. 7. Locus of wheel center for ideal disk wheel

For a realistic wheel radius and wave amplitude the effect is hardly visible, Fig. 7, left part.

Thus we show the same dependence for a much smaller wheel (10 times reduced radius), right part.

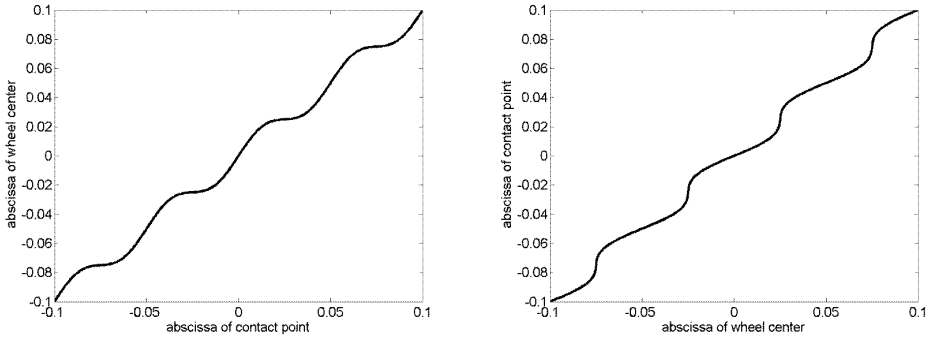

Fig. 8. Horizontal position of center (left: steady rolling, right: constant speed)

4.1.2. Effects and Options

Fig. 8 shows the consequences of the geometric contact condition. Ideal rolling at constant horizontal speed leads to a high variation in rotational speed, constant revolutions require heavy variation of horizontal speed.

Both induce extreme vertical or horizontal accelerations, see Fig. 10, right, where we assumed a constant horizontal speed of 36 m/s.

Interesting – from the view point of wave generation – is also the speed of the moving contact point, cf. Fig. 10, left.

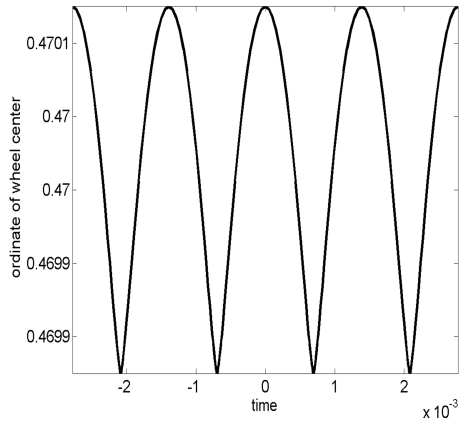

Fig. 9. Vertical position (steady forward motion)

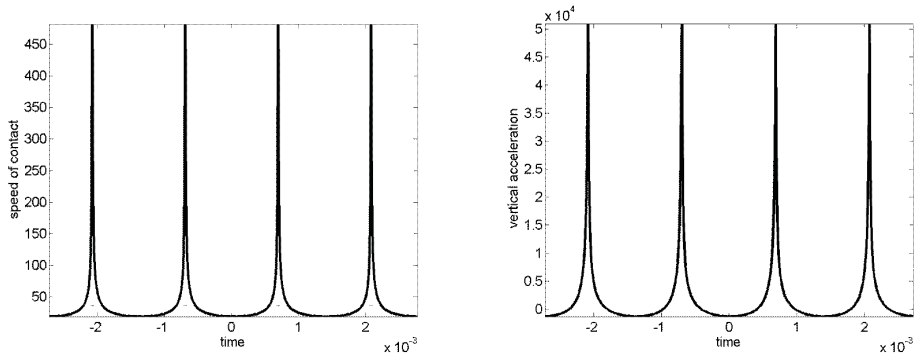

Fig. 10. Left: Horizontal speed of contact point (steady forward motion); Right: Vertical acceleration (steady forward motion)

4.2. Dynamics

4.2.1. Equation of Motion and Parameters

We assume the following equations

$$x_c' = V_0 \tag{16}$$

$$y_c' = v_y \tag{17}$$

$$v_y' = F_y/m \tag{18}$$

$$\alpha' = \omega \tag{19}$$

$$\omega' = M/I \tag{20}$$

In addition to the previously given parameters defining the existing corrugations, the following values, Table 3, were used in the numerical calculations:

Table 3

Parameters of dynamical model

mass of wheel	m	1000 kg
inertial moment of wheel	I	850 kg m
load on wheel	L	200000 N
elasticity of contact	k	1e10 N/m
normal damping in contact	d	4e5 Ns/m
friction parameter	μ	0.12

The most tricky part, however, is the modeling of the normal force F_y and the angular moment M, which define the accelerations of the vertical and angular positions.

Remark 2 *As control motion, we impose a prescribed horizontal motion of the center of the wheel. As alternatives, a prescribed total speed of the wheel center, a prescribed horizontal force or total force could be easily considered. In a forthcoming paper we plan to study a wheel suspended by means of springs and dampers to a simple bogie.*

In general, there is a considerable influence of the control motion and the suspension on the resulting trajectories.

4.3. Numerical Results

Here, we do experiments with prescribed horizontal speed. We vary speed and contact damping.

On Fig. 11, we assume minimal damping, and show trajectories for very small speeds. On Fig. 12, we assume medium damping, and show trajectories from 8m/s to 40m/s. Finally, in Fig. 13, we show results for the same speeds, but large damping.

All calculations are performed for an amplitude of 1/8 mm on the wheel, ideal track. This is just below the critical amplitude, where convexity is lost.

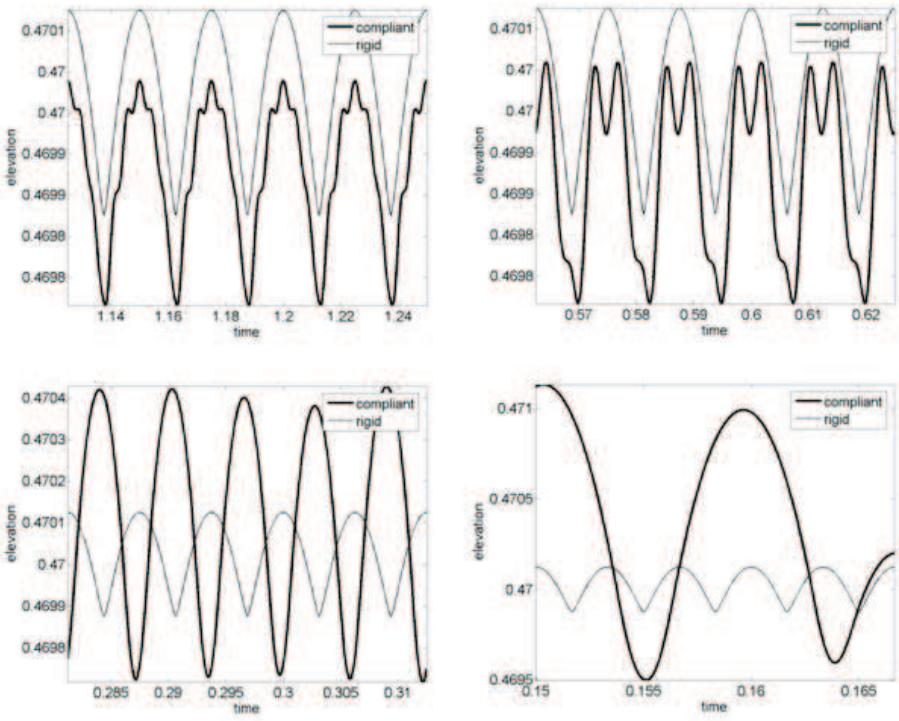

Fig. 11. Vertical position for small damping

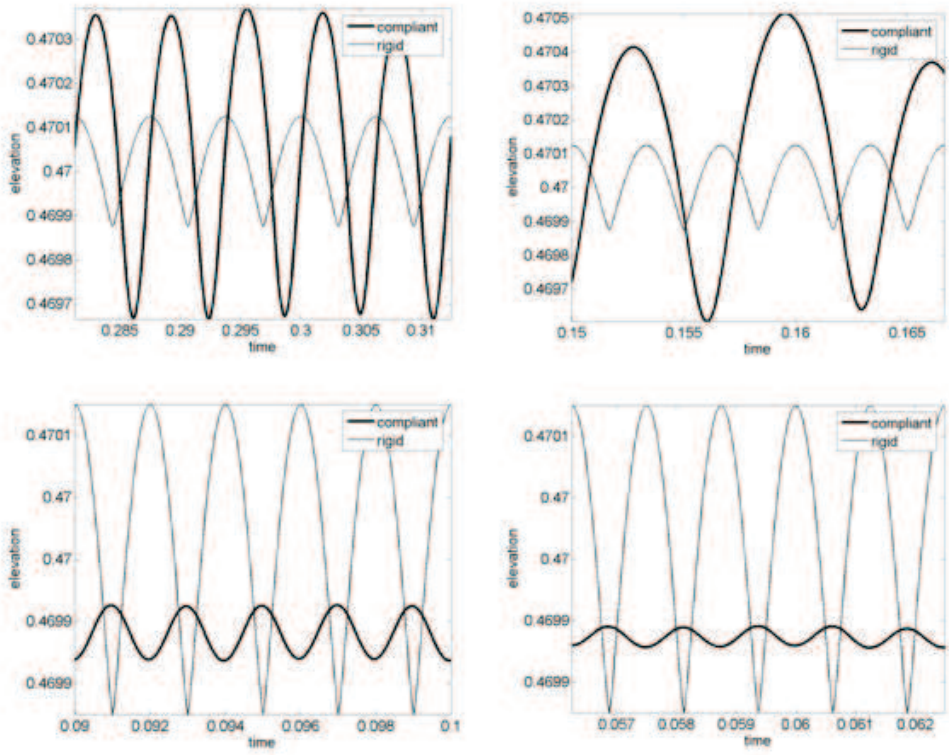

Fig. 12. Vertical position for realistic damping

Remark 3 *At small horizontal speeds (2,4,8,15 m/s), the wheel center moves along a parallel to the curve obtained by the rigid body approach, the vertical shift being the value of the elastic approach (1e-4 m).*

Without or with small damping, at very low speed parametric excitation causes considerable deviations from the quasi-static trajectory, which finally leads to bouncing – lift off, free-flight phases and bumping back onto the rail. At small damping, higher speed, the phases of penetration are rare, free flight is prevalent. Motion becomes chaotic with increasing speed.

Remark 4 *For reasonable damping, we obtain again bouncing, but synchronized with the corrugation pattern. Lift off starts behind the maximum elevation of the rigid constraint, the track is hit again behind the minimum.*

With increasing speed (8,15,25,40 m/s for both Figs. 12 and 13), the motion tends to anti-phase mode. The wheel is lowest, where it would be highest according to the rigid constraint. So, the highest normal force occurs at the humps of the radius – which is in principle good news.
With increasing speed, the amplitude of the wheel center motion decreases.

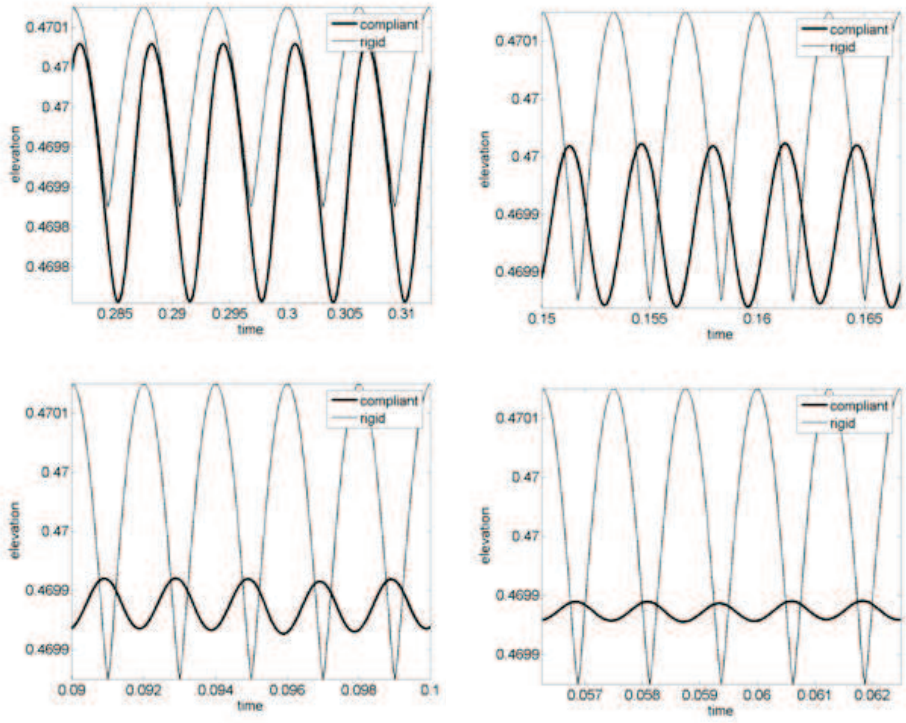

Fig. 13. Vertical position for large damping

At very large damping, see Fig. 13, a speed may be found, for which the wheel center moves smoothly along its rigid constraint.

5. Conclusions

For the contact of corrugated wheels and rails, we observe a considerable variation of the speed of the contact point around the horizontal speed of the wheel.

The critical speed – from the point of view of the theory of traveling forces on supported beams – may be exceeded for very moderate speeds of wheel motion. Above certain levels of expression of the corrugation patterns lift off may occur, which is followed by an impact.

Practically, a rigid constraint model is rather not realistic, viscoelastic oscillations around the quasi-static trajectory are most intriguing.

By cumulating the energy dissipated at impact points, the evolution of the corrugation pattern may be simulated. Effects of abrasion were studied elsewhere and are left out of this discussion. Calculations for wavy track are underway.

References

1. Arnold M., Frischmuth K.: Solving problems with unilateral constraints by DAE methods. Mathematics and Computers in Simulation 47:47-67, 1998.
2. Bogacz R., Frischmuth K.: Computer Simulation of slip wave generation, Proceedings of the 8th PTSK, Gdańsk, 2001.
3. Bogacz R., Frischmuth K.: Simulation of wheelset in curved track. Machine Dynamics Problems, 25 No 3/4 2002.
4. Frischmuth K.: Regularization methods for non-smooth dynamical problems, [in:] R. Bogacz, G. P. Os- termeyer and K. Popp (Editors), Dynamical Problems in Mechanical Systems IV, Proceedings of the 4th Polish-German Workshop, July 30 – August 4, 1995 in Berlin, IPPT-PAN, Warsaw, 99–108, 1996.
5. Frischmuth K.: On the numerical solution of rail-wheel contact problems. J. Theoretical and Applied Mechanics, 34, 1, 7–15, 1996.
6. Frischmuth K.: Wear models with internal state parameters, Machine Dynamics Problems, 24, No. 1, pp. 79–86, 2000.
7. Frischmuth K.: Contact, motion and wear in railway mechanics, Journal of Theoretical and Applied Mechanics, 3, 39, 2001.
8. Frischmuth K.: Numerical methods for evolving manifolds, and applications in rail-wheel contact mechanics, [in:] Selected topics in Geometry and Mathematical Physics, Vol. 1, 161-187, 2002.
9. Frischmuth K., Langemann D.: Distributed numerical calculations of wear in the wheel-rail contact, in: System Dynamics and Long-Term Behaviour of Railway Vehicels, Track and Subgrade (Eds. Popp, Schiehlen), Springer (2002).
10. Bogacz R., Krzyżński T., Popp K.: On generalization of Mathews' problem of the vibration of a beam on elastic foundation, Z.angew. Math. Mech. 69, 1989, 243-252.
11. Bogacz R., Frischmuth K.: Vibration in Sets of Beams and Plates Induced by Traveling Loads, Archive of Applied Mechanics, 2008 pp. xx.
12. Jensen J.C., Slivsgaard E.: Modelling of raiway vehicles using elastic contact and moveable track, [in:] Proc. First Workshop on Dynamics of Wheel–Rail Systems. Rostock 1994, pp. 19-23.
13. Bogacz R., Kowalska Z.: Computer simulation of the interaction between a wheel and a corrugated rail, Eur. J. Mech. A/Solids 20, 2001, pp. 673–684.
14. Bogacz R., Frischmuth K.: Models of surface pattern development in rolling contact, X Internat. Conf. TRANSCOMP 2006 Vol. I, pp. 59–64.
15. Kowalska Z.: Vibro-impacts induced by irregular rolling surfaces of railway rails and wheels Journalof Theoretical and Applied Mechanics, 46, 1, pp. 205–221, Warsaw 2008.
16. Bogacz R., Chudzikiewicz A., Frischmuth K.: Friction, wear and heat, [in:] L. Bobrowski and A. Tylikowski (eds.) Simulation in R&D., Warsaw, 2005 pp.67-76.